Dynamical Analysis and Synthesis of Inertia-Mass Configurations of a Spacecraft with Variable Volumes of Liquids in Jet Engine Tanks

ANTON V. DOROSHIN, MIKHAIL M. KRIKUNOV

Space Engineering Department (Division of Flight Dynamics and Control Systems)
Samara State Aerospace University (National Research University)
SSAU, Moscowskoe shosse 34, Samara, Russia 443086
RUSSIAN FEDERATION
doran@inbox.ru; Krikunov_MM@mail.ru

Abstract: **-** In the article the attitude motion of a spacecraft with variable mass/structure is considered at the variability of the volume of liquids (the fuel and the oxidizer) in tanks of the jet engines. The variability of the liquid's volume is occurred under the action of systems of the extrusion of liquids by the pressure creation and, as a result, by the diaphragm (a thin soft foil) deformation inside the fuel/oxidizer tank. The synthesis of the attitude dynamics is fulfilled by the change of directions of the extrusion of the liquids in tanks – this modifies the inertia-mass parameters (their corresponding time-dependencies) and affects the final motion dynamics. Here we showed that the extrusion in the lateral radial "outside" direction is most preferable in comparison with the longitudinal extrusion (in the direction of jet-vector). It means that the precession cone of the longitudinal axis of the spacecraft (the axis of the jet-engine reactive thrust) is "twisted up" to the precalculated necessary direction of jet-impulse, and it has not "untwisted" phases. This scheme of the liquid extrusion is dynamically optimal, because it allows to improve the active inter-orbital maneuver by the natural/uncontrolled/passive way.

Key-Words: - Spacecraft; Variability of the Volume of Liquids; Tanks of the Jet-Engines; Attitude Dynamics; The Curvature Method; Precession Motion

1. Introduction.

The task of the spacecraft (SC) attitude dynamics investigation/synthesis at the implementation of the active maneuvers is one of the main tasks of the space flight mechanics.

This task is considered in different formulations taking into account many different aspects, including regimes of controlled/uncontrolled regular/chaotic attitude motion of rigid and flexible SC with constant and variable inertia-mass parameter, an implementation of the attitude reorientation using mechanical actuators and thrusters, etc. The corresponding research results are described in many works [e.g. 1-44], which are not limited by the indicated references list.

In this research we give the short description of some features of the SC with two types of the liquids extrusion in spherical jet-engines tanks. We will consider symmetrical bunches of four spherical tanks (for example, two tanks contain the fuel, and other two tanks contain the oxidizer). This scheme is usually used in the upper stages and boosters configurations. So, let us describe the scheme with spherical tanks (fig.1).

The attitude motion of the SC is considered in this research as the angular motion around the fixed point, coincided at the initial time-moment with the initial position of the center of mass of SC [9-11].

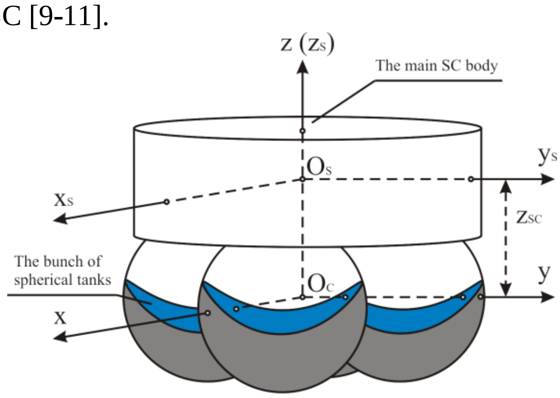

Fig.1 *The bunch/block of spherical tanks*

This mechanical model allows applying the simple type of the definition of the internal geometry (inertia-mass geometry) and corresponding variable inertia-mass parameters.

So, the mathematical model of the attitude motion was built in the works [9-11] for the case of dual-spin spacecraft (with four degrees of freedom). This model represents the dynamical equations connected with the angular momentum components, and we will use this model in this article without essential modifications at the fixing/elimination of the relative rotation of coaxial bodies.

2. The mathematical model of motion

Let us investigate the free (without the action of any external perturbations) attitude motion of the spacecraft with the variable volume of the liquids (the fuel/oxidizer) in the tanks. The equations [9-11] in the considering case can be reduced to the simple form:

$$\begin{cases} A(t)\dot{p}+\left(C(t)-B(t)\right)qr=0, \\ B(t)\dot{q}+\left(A(t)-C(t)\right)pr=0, \\ C(t)\dot{r}+\left(B(t)-A(t)\right)pq=0, \end{cases} \quad (1)$$

where $A(t)=B(t), C(t)$ — the variable inertia moments of the SC calculated relatively the point O; and p, q, r — are the angular velocity's components. The total values of the inertia moments are summarized by the terms

$$A(t)=A_S+A_T(t)-M(t)z_C^2(t),$$
$$C(t)=C_S+C_T(t),$$

where A_S, C_S are the constant parts of the inertia moments corresponding to the rigid part of the SC structure (the main SC body including the empty tanks), and A_T, C_T – are the varied (depending on time) parts corresponding to inertia moments of the tanks with momentary "current-freezing" forms of liquids ($M(t)$, $z_C(t)$ – the current values of the mass of the SC and the coordinate of the current position of the center of mass ($z_C(0)=0$).

The angular/attitude/spatial orientation of the SC (fig.2) is described by the Euler's type angles ($\psi\to\gamma\to\varphi$).

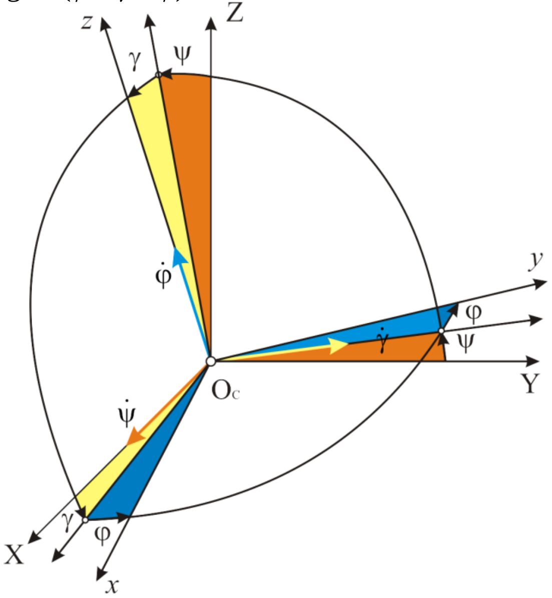

Fig. 2 *The spatial orientation angles*

The kinematical equations for the spatial angles are follows:

$$\begin{aligned} \dot{\gamma} &= p\sin\varphi+q\cos\varphi, \\ \dot{\psi} &= \frac{1}{\cos\gamma}\left(p\cos\varphi-q\sin\varphi\right), \\ \dot{\varphi} &= r-\frac{\sin\gamma}{\cos\gamma}\left(p\cos\varphi-q\sin\varphi\right). \end{aligned} \quad (2)$$

It will be quite useful to make the change of the variables [9-11]:

$$\begin{aligned} p &= G(t)\sin F(t), \\ q &= G(t)\cos F(t). \end{aligned} \quad (3)$$

Then the dynamical equations (1) can be rewritten:

$$\begin{cases} \dot{F} = -\dfrac{1}{A(t)}\left[\left(C(t)-A(t)\right)r\right], \\ G=\text{cosnt}>0, \qquad r=\text{const} \end{cases} \quad (4)$$

Let us consider the case of the attitude motion of the gyroscopic stabilized SC with the predominance of the longitudinal component of the angular velocity (r) in comparison with the equatorial component:

$$\varepsilon=\sqrt{p^2+q^2}\Big/|r|<<1.$$

In this case we can rewrite the kinematical equations in the simplified form [9-11]:

$$\begin{aligned} &\dot{\gamma}\cong G\cos\Phi(t), \quad \dot{\psi}\cong G\sin\Phi(t), \\ &\dot{\varphi}\cong r, \qquad \Phi(t)=F(t)-\varphi(t). \end{aligned} \quad (5)$$

where $\Phi(t)$ is the phase of spatial oscillations. The equations (5) allow to consider the dynamics of the SC longitudinal axis ($O_C z$) with the help of the phase point (the apex of the axis $O_C z$) at the phase-plane $\{\psi\text{-}\gamma\}$. Then the velocity (V) and the acceleration (W) of this phase point, and the curvature (k) of the corresponding trajectory of this point are:

$$V_\gamma=\dot{\gamma},\ V_\psi=\dot{\psi},\ W_\gamma=\ddot{\gamma},\ W_\psi=\ddot{\psi}.$$
$$k^2=\left(\ddot{\gamma}\dot{\psi}-\ddot{\psi}\dot{\gamma}\right)^2\Big/\left(\dot{\gamma}^2+\dot{\psi}^2\right)^3=\dot{\Phi}^2/G^2.$$

For the analysis/synthesis of the dynamics we can apply the qualitative "curvature" method [9-11], which is very useful for the optimization of the form of the hodograph vector of the jet-thrust direction of the SC at the gyroscopic attitude stabilization. This method is based on the evaluation of the roots of the "evolution function" $\tilde{P}(t)$, which describes the evolution of the curvature of the trajectory of the phase point (excluding the multipliers of constant signs):

$$\tilde{P}=\text{const}\cdot k\dot{k}=\dot{\Phi}\ddot{\Phi}G-\dot{G}\dot{\Phi}^2. \quad (6)$$

Taking into account the equations (4) we can rewrite the expression for the "evolution function" (excluding the multipliers of constant signs):

$$\tilde{P}(t) = \dot{C}A - \dot{A}C \qquad (7)$$

The intervals of the positive sign conservation of this function correspond to the SC's monotonous phases of the angular motion with twisting (Fig.3-a) sections of the longitudinal axis (the trust direction) hodograph (on the plane of parameters γ-ψ). The alternation of the signs of the function (the existence of real roots) results in the alternation of the hodograph's phases. At the Fig.3 it is possible to see the clotoid (Fig.3-b, that corresponds to the existence of one root of $\tilde{P}(t)$) and the complex phase-alternation-spiral (Fig.3-c, that corresponds to the existence of many roots of $\tilde{P}(t)$).

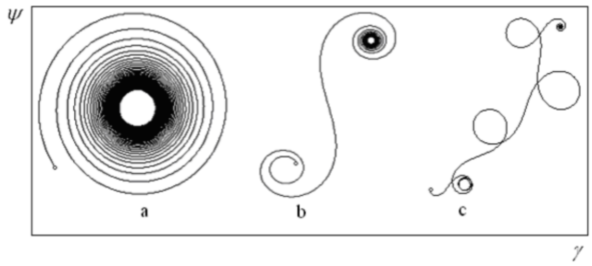

Fig.3 *The hodographs of the longitudinal SC axis* ($O_c z$) *on the tangential plane {ψ-γ}*

These evolutions of the hodographs' affect the inter-orbital transitions' implementation [9] due to the corresponding "travel" of the trust-vector (Fig.4) with the accumulation of the impulses' error.

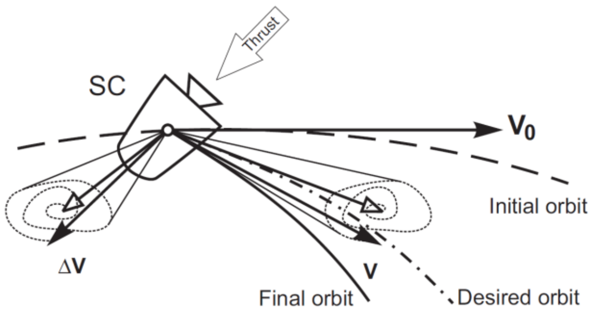

Fig.4 *The influence of the attitude motion on the inter-orbital transitional maneuver*

So, in the purposes of the "positive" dynamics (with the inside twisting hodograph (Fig.3-a)) synthesis the function $\tilde{P}(t)$ has to be positive on the whole time-interval of the motion [9-11].

The following references' frames are used in the research:

1. $O_C xyz$ — the main coordinates frame connected to the main axes of the SC (Fig.1) with the origin in the point O_C of the SC coincided with the initial position of the system's mass center.
2. $O_S x_S y_S z_S$ — the frame connected to the rigid part of the system's structure (the SC without the tanks). Moreover, the frame axes (Fig.1) are collinear with the axes of the main coordinates frame $\left(x \uparrow\uparrow x_S;\ y \uparrow\uparrow y_S;\ z \equiv z_S\right)$.
3. $Ox_0 y_0 z_0$ — the frame geometrically connected to the tank (coinciding with its main axes) with the origin in the geometrical center of the tank (Fig.5).

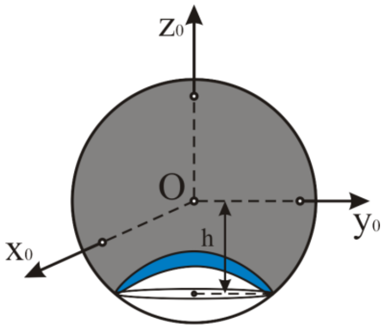

Fig. 5. *The frame connected with the tank*

4. $O_T x_T y_T z_T$ — the frame (Fig. 6) connected to the bunch of the tanks with the origin in the geometrical center of the tanks bunch.

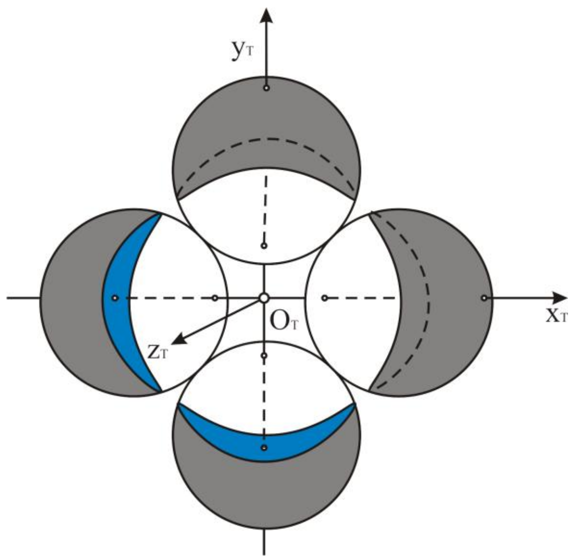

Fig. 6 *The frame connected with the geometrical center of the tanks bunch*

5. $O'x'y'z'$ — the frame with axes which is collinear to the axes $O_C xyz$, and with the origin in the "lowest" point of the SC *O*.

Now we can calculate the inertia moments:

$$A(t) = A_S + A_T(t) - Mz_C^2, \quad C(t) = C_S + C_T(t), \tag{8}$$

where A_S, C_S — are the constant parts of the inertia moments corresponding to the rigid part of the SC structure (the main SC body with the empty tanks), and A_T, C_T – are the varied parts corresponding to inertia moments the tanks (including momentary "current-freezing" forms of liquids and the empty tanks) calculated in the frame $O_C xyz$; $M = M(t)$ — is the mass of SC in the current time-moment; $z_C = z_C(t)$ — is the current coordinate of the SC mass center, that can be calculated as follows

$$z_C = z'_{C_0} - z'_C, \tag{9}$$

$$M = m_S + m_{ET} + m_T(t), \tag{10}$$

where z'_C — is the coordinate of the position of the mass center at present time in the frame $O'x'y'z'$ and $z'_{C_0} = z'_C(0)$ — the coordinate of the center of mass at the initial time moment (also in the frame $O'x'y'z'$); m_S — the constant mass of the rigid part of the SC without the empty tanks; m_{ET} - is the mass of the empty tanks; $m_T(t)$ — is mass of liquids in the tanks at the current time.

The recalculation of the inertia moments of the rigid part of the SC without empty tanks can be fulfilled as follows:

$$A_S = A_{S0} + m_S z_{SC}^2, \quad C_S = C_{S0},$$

где A_{S0}, C_{S0} — the inertia moments of the rigid SC body in the frame $O_S x_S y_S z_S$, with the defined/known values; $z_{SC} = \text{const}$ — is the distance between the mass center of the rigid SC body and point O_C (the initial position of the mass center of the system with the filled tanks).

The inertia moments of the tanks can be find in the form:

$$A_T = A_{T0}(t) + m_T z_T^2, \quad C_T = C_{T0}(t), \tag{11}$$

where $A_{T0}(t)$, $C_{T0}(t)$ — are the inertia moments calculated in the frame $O_T x_T y_T z_T$, and $z_T = z_T(t)$ — is the distance between the mass center of the tanks bunch and the point O_C.

The value z_{SC} also formally follows from the expression:

$$z_{SC} = z'_{C_0} - z'_{SC}, \tag{12}$$

where z'_{KC} — the position of the mass center of the SC's rigid part/structure in the frame $O'x'y'z'$. The value z_T satisfies to the equality:

$$z_T = z'_{C_0} - z'_T, \tag{13}$$

where z'_T is the position of the mass center of the bunch of the tanks in the frame $O'x'y'z'$.

Now it is possible to formally find the position of the system mass center in the frame $O'x'y'z'$:

$$z'_C = \frac{1}{M}\left(z'_{SC} m_S + z'_T m_T\right), \tag{14}$$

For example, we consider the SC with the height of the main rigid part H_S and with the bunch of the tanks with the diameter a. Then we have

$$z'_{SC} = \frac{1}{m_{SC}}\left[m_S\left(a + H_S / 2\right) + m_{ET}\frac{a}{2}\right], \quad m_{SC} = m_S + m_{ET}. \tag{15}$$

The defined geometrical values undoubtedly depend on the selected shapes of the tanks. In turn, it is clear that the tanks can have different shapes (spheres, cylinders, conical parts, compound forms). Also methods of the liquids extrusion from the tanks differ from each other. For example, the fuel-tank pressurization with the tissue-type or foil-type diaphragms is quite useful.

Let us consider in this research the spherical tanks equipped with the extrusion systems with the hemispherical foil-type diaphragms edge-stiffened in the line of the internal diameter of the tank – the pressure is injected into the gap between the diaphragm and the internal tank's wall, then the irretrievable foil's deflection forms. Such types of the diaphragms allow to fulfill the liquid extrusion without formation of the free liquid's surface at the conservation of the current reached lens-shaped deformity (Fig.5) of the foil (this lens-shaped deformity/deflection rises with the time, and in limit it coincides with the complete spherical tank).

So, the main considering task is the search of the tanks dispositions providing the realization of the "positive" attitude dynamics of the SC on active sections of the trajectory/orbital motion, when the accuracy of the jet propulsion inter-orbital impulse increases by natural way during the SC precession motion with the spiral-convolving hodograph of the SC longitudinal axis (coinciding with the vector of the jet-engine thrust).

Here the most important part of the task is the selection of the direction of the internal motion of the extrusive diaphragms inside the tank. We can dispose the extrusive diaphragm inside the tank along the thrust vector ("downward extrusion" – Fig.1); or the diaphragms can be disposed in the orthogonal direction and the liquid will be extruded radially outwards ("radial extrusion" – Fig.6).

It is possible to expect that the attitude dynamics at the radial extrusion will differ from the downward one. Let us to make an investigation of this question.

3. The comparative modeling of the extrusions

3.1. The radial extrusion

Let us consider the attitude motion at the radial extrusion realization (Fig.6).

The inertia moments $A_{T0}(t)$ and $C_{T0}(t)$ in the frame $O_T x_T y_T z_T$ can be calculated as follows:

$$A_{T0}(t) = 2A_F + 2C_F + 2m_T(l^2 - r^2), \quad (16)$$

$$C_{T0}(t) = 4A_F + 4m_T(l^2 - r^2), \quad (17)$$

where $A_F = A_F(t)$ and $C_F = C_F(t)$ — are the inertia moment of the current volume of the liquid in the single tank in the frame $Ox_0y_0z_0$ (Fig.5); $l = l(t)$ — is the distance between the point O_T and the mass center of the current volume of the liquid in one tank along $O_T x_T$; $r = r(t)$ — the distance between the geometrical center of the of the single tank and the mass center of the current volume of the liquid in one tank along $O_T x_T$.

We must additionally comment the process of the liquid extrusion: the foil-type diaphragm deforms under the action of the pressure such way, that the created empty space (between the internal tank's wall and the sagged diaphragm) always has symmetrical lens-type shape (Fig.5).

In this case the inertia moments (16) and (17) have the concretized form:

$$A_F = I_0 - \frac{\pi\rho}{5}\left(\frac{8}{3}R^5 + \frac{1}{4}h^5 - \frac{15}{4}R^4 h + \frac{5}{6}R^2 h^3\right) - 2m_1 h(h - z_{C1}), \quad (18)$$

$$C_F = I_0 - \frac{\pi\rho}{5}\left(\frac{8}{3}R^5 - h^5 - 5R^4 h + \frac{10}{3}R^2 h^3\right), \quad (19)$$

where I_0 − the inertia moment of the single full spherical tank completely filled with the liquid; ρ − the liquid density; R − the radius of the tank; $h = h(t)$ − the distance between the geometrical center of the tank and the median plane of the empty lens-type space (Fig.5); m_1 − the mass of the current extruded volume of the liquid in the tank; z_{C1} − the distance between the geometrical center of the of the single tank and the spherical segment (one half of the "lens").

$$I_0 = \frac{2}{5}m_0 R^2, \; m_0 = \frac{4}{3}\pi\rho R^3 \quad (20)$$

$$m_1 = 2\pi\rho(R-h)^2\left(\frac{2}{3}R + \frac{1}{3}h\right) \quad (21)$$

$$z_{C1} = \frac{3}{4}\frac{(R^2 - h^2)^2}{2R^3 - 3R^2 h + h^3} \quad (22)$$

The value *l* and *r* are calculated as:

$$r(t) = \frac{m_1}{m_0 - m_1}h(t) \quad (23)$$

$$l(t) = R\sqrt{2} - r(t) \quad (24)$$

$$z'_T = R$$

Let us consider the linear time-dependence of $h(t)$:

$$h(t) = h_0 - h_1 t.$$

Now we can plot the graph (Fig.7) for the function of the thrust's hodograph curvature $\tilde{P}(t)$ at the parameters from the table 1.

Table 1 – *The parameters of the SC*

The parameter	The value
ρ, kg/m^3	780
h_0, m	1
h_1, m/s	0.025
R, m	1
A_S, kg·m^2	8600
C_S, kg·m^2	18600
m_S, kg	100
H_S, m	2

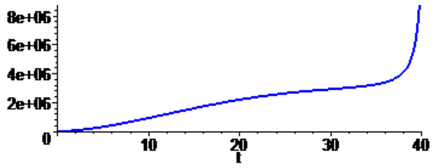

Fig.7 *The thrust's hodograph curvature function* $\tilde{P}(t)$ *at the radial extrusion:*
the function is positive;
and it has no roots

As we can see, the thrust's hodograph curvature function is positive and has no roots. The corresponding hodograph is presented at the figure (Fig.8) – as it was expected this hodograph is spiral-convolving curve and the corresponding attitude dynamics is also "positive" in the above mentioned sense.

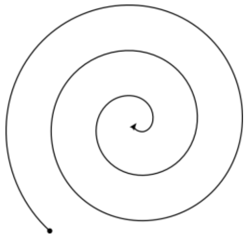

(a)

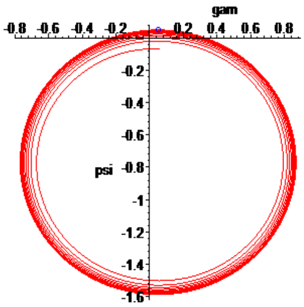

(b)

Fig.8 *The thrust's hodograph at the radial extrusion of the liquids in the tanks:*
(a) – the schematic monotone type of the hodograph
(b) – the real implementation
(G_0=1.5 [1/s]; F_0=0; r=2 [1/s]; the small blue circle corresponds to the initial position)

3.2. The downward extrusion

Let us now consider the second type of extrusion – the "downward extrusion" (like at the Fig.1). the inertia moments $A_{T0}(t)$ and $C_{T0}(t)$ can be calculated from (11):

$$A_{T0}(t) = 4A_F + 2m_T d^2, \qquad (25)$$

$$C_{T0}(t) = 4C_F + 4m_T d^2, \qquad (26)$$

where $d = R\sqrt{2} = \text{const}$ — is the distance between the point O_T and the geometrical center of the tank.

The inertia moments (16) and (17) in considering case have the form (18) and (19). Also the following values take place:

$$z'_T(t) = R - \frac{m_1(t)}{m_0 - m_1(t)} h(t) \qquad (27)$$

Then the evolution functions $\tilde{P}(t)$ (at the conditions from tab.1) is sign-alternating and has real roots (Fig.9).

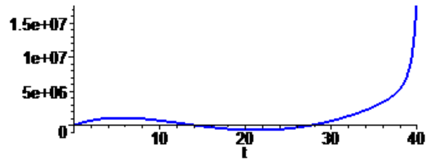

Fig.9 *The thrust's hodograph curvature function* $\tilde{P}(t)$ *at the downward extrusion:*
the function is sign-alternating;
and it has two roots in the open interval t=(0,T)

The corresponding hodograph is presented at the figure (Fig.10) – as it was expected, this hodograph is not monotonously twisting, and it has the first twisting phase (the black section of the schematic hodograph – Fig.10-a), the second untwisting phase (the red section of the schematic hodograph – Fig.10-a) and the third twisting phase (the blue section of the schematic hodograph – Fig.10-a). So, the untwisting phase is realized in the time-interval t=(12..28) where the evolution function is negative) – it characterizes the attitude dynamics as not-positive because inside the "untwisting phase's" time-interval the thrust defocusing takes place, and corresponding jet-impulse is "nebulized in parasite directions".

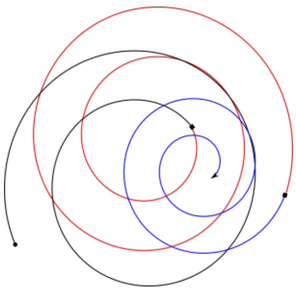

(a)

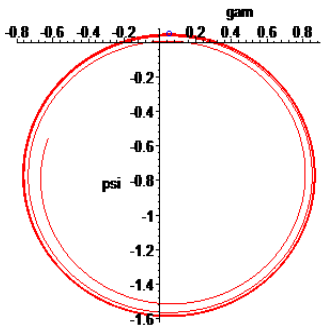

(b)

Fig.10 *The thrust's hodograph at the downward extrusion of the liquids in the tanks*
(a) – the schematic three-section type of the hodograph
(b) – the real implementation

So, as we can see, the radial type of the extrusion system is optimal in the dynamical sense, when the accuracy of the inter-orbital jet impulse increases by the natural way during the SC precession motion with the spiral-convolving hodograph of the SC longitudinal axis (coinciding with the vector of the jet-engine thrust), that in its turn corresponds to the precessional motion with the twisting nutation cone.

The attitude dynamics at the downwards extrusion is not positive, and we can recommend to change this type of extrusion system on the radial one – this is the main applied/technical result of the fulfilled research.

Conclusion

The attitude dynamics of the SC with the variable volume of the liquids (the fuel and the oxidizer) in the bunch of spherical tanks was investigated based on the qualitative method for the analysis of the curvature of phase trajectories. Two schemes of the extrusion system (the radial and the downward extrusion) were considered.

As it was shown, the attitude dynamics at the downwards extrusion is not positive, that results in the complex trajectory of the apex of the longitudinal axis of the SC (coinciding with the thrust vector of the jet-engine) – this trajectory represents the complex spiral with the twisted and untwisted sections, and the corresponding attitude motion negative affects the jet-engine-impulse.

Owe of the main results of the work is the recommendation of using of the radial extrusion scheme instead the downward scheme. The radial extrusion scheme is optimal in the dynamical sense, when the accuracy of the inter-orbital jet-impulse increases by the natural way during the SC precession motion with the spiral-convolving hodograph of the SC longitudinal axis (coinciding with the vector of the jet-engine thrust), that in its turn corresponds to the precessional motion with the twisting nutation cone.

So, the work additionally confirms the fact that the attitude dynamics of the SC with the variable mass/structure strongly affects its orbital motion.

References

1. A. A. Kosmodem'ianskii, A Course in Theoretical Mechanics, Part 2, Jerusalem, Published for the National Science Foundation, Washington, by the Israel Program for Scientific Translations, 1963.
2. J. Wittenburg, Dynamics of Systems of Rigid Bodies. Stuttgart: Teubner, 1977.
3. F.R. Gantmaher, L.M. Levin, The Theory of Rocket Uncontrolled Flight, Fizmatlit, Moscow, 1959.
4. M. Iñarrea, V. Lanchares, Chaotic pitch motion of an asymmetric non-rigid spacecraft with viscous drag in circular orbit, Int. J. Non-Linear Mech. 41 (2006) 86–100
5. V. Lanchares, M. Iñarrea, J.P. Salas, Spin rotor stabilization of a dual-spin spacecraft with time dependent moments of inertia, Int. J. Bifurcation Chaos 8 (1998) 609–617.
6. M. Iñarrea, V. Lanchares, Chaos in the reorientation process of a dual-spin spacecraft with time-dependent moments of inertia, Int. J. Bifurcation and Chaos. 10 (2000) 997-1018.
7. M. Iñarrea, V. Lanchares, V.M. Rothos, J.P. Salas. Chaotic rotations of an asymmetric body with time-dependent moments of inertia and viscous drag. International Journal of Bifurcation and Chaos, Vol. 13, (2003), 393-409.
8. M. Iñarrea, V. Lanchares, Chaotic pitch motion of an asymmetric non-rigid spacecraft with viscous drag in circular orbit, Int. J. Non-Linear Mech. 41 (2006) 86–100.
9. A.V. Doroshin, Analysis of attitude motion evolutions of variable mass gyrostats and coaxial rigid bodies system, International Journal of Non-Linear Mechanics. Volume 45, Issue 2 (2010) 193-205.
10. A.V. Doroshin, Synthesis of Attitude Motion of Variable Mass Coaxial Bodies, WSEAS TRANSACTIONS on SYSTEMS AND CONTROL, Volume 3 (2008) 50-61.
11. A.V. Doroshin, Evolution of the precessional motion of unbalanced gyrostats of variable structure, Journal of Applied Mathematics and Mechanics, Volume 72, Issue 3 (2008) 259-269.
12. V.S. Aslanov, A.V. Doroshin, G.E. Kruglov, The Motion of Coaxial Bodies of Varying Composition on the Active Leg of Descent, Cosmic Research, Vol.43, No. 3 (2005) 213-221.
13. V.S. Aslanov, V.V. Yudintsev, Dynamics and control of dual-spin gyrostat spacecraft with changing structure. Celestial Mechanics and

Dynamical Astronomy, Volume 115, Issue 1 (2013) 91-105.

14. V.S. Aslanov, The Dynamics and Control of Axial Satellite Gyrostats of Variable Structure. Proceedings of 1st IAA Conference on Dynamics and Control of Space Systems Porto, Portugal 19-21 March 2012, p. 41-54.
15. A.V. Doroshin, Phase Space Research of One Non-autonomous Dynamic System, Proceedings of the 3rd WSEAS/IASME International Conference on DYMAMICAL SYSTEM and CONTROL. Arcachon, France (2007) 161-165.
16. A.V. Doroshin, M.M. Krikunov, Attitude dynamics of a spacecraft with variable structure at presence of harmonic perturbations, Applied Mathematical Modelling, Volume 38, Issues 7–8 (2014) 2073-2089.
17. V.L. Balakin, A.V. Doroshin, M.M. Krikunov, SYNTHESIS OF DYNAMIC MODES OF ATTITUDE MOTION OF SPACECRAFT WITH SOLID PROPELLANT ROCKET ENGINE, The Bulletin of the Samara State Aerospace University (Vestnik SGAU), #5-36 (2012) 13-19.
18. A.V. Doroshin, Exact solutions in attitude dynamics of a magnetic dual-spin spacecraft and a generalization of the Lagrange top, WSEAS Transactions on Systems 12 (10) (2013) 471 – 482.
19. A.V. Doroshin, Exact solutions for angular motion of coaxial bodies and attitude dynamics of gyrostat-satellites, International Journal of Non-Linear Mechanics 50 (2013) PP. 68 – 74.
20. A.V. Doroshin, Modeling of chaotic motion of gyrostats in resistant environment on the base of dynamical systems with strange attractors. Communications in Nonlinear Science and Numerical Simulation, Volume 16, Issue 8 (2011) 3188–3202.
21. A.V. Doroshin, Heteroclinic dynamics and attitude motion chaotization of coaxial bodies and dual-spin spacecraft, Communications in Nonlinear Science and Numerical Simulation, Volume 17, Issue 3 (2012) 1460–1474.
22. A.V. Doroshin, Homoclinic solutions and motion chaotization in attitude dynamics of a multi-spin spacecraft Communications in Nonlinear Science and Numerical Simulation 19(7) (2014) 2528 – 2552.
23. A.V. Doroshin, Chaos and its avoidance in spinup dynamics of an axial dual-spin spacecraft, Acta Astronautica 94(2) (2014) 563 – 576.
24. A.V. Doroshin, Spinup-capture dynamics of multi-rotor nanosatellites and somersaulting robots, (2013) Proceedings of 2013 Science and Information Conference, SAI 2013 PP. 613 – 617.
25. Filippo Neri, Traffic packet based intrusion detection: decision trees and generic based learning evaluation. WSEAS Transactions on Computers, WSEAS Press (Wisconsin, USA), issue 9, vol. 4, 2005, pp. 1017-1024.
26. Filippo Neri, Software agents as a versatile simulation tool to model complex systems. WSEAS Transactions on Information Science and Applications, WSEAS Press (Wisconsin, USA), issue 5, vol. 7, 2010, pp. 609-618.
27. Antonio Gil V. De Brum, Márcio A. A. Fialho, M. L. Selingardi, Nilton D. Borrego, José L. Lourenço, The Brazilian Autonomous Star Tracker – AST, WSEAS Transactions on Systems 12 (10) (2013) 459-470.
28. C. F. de Melo, F. Neri, An Introduction to the Special Issue on Orbital Dynamics and Spacecraft Attitude Control, WSEAS Transactions on Systems 12 (10) (2013) 457-458.
29. Kozlov V. V. Methods of qualitative analysis in the dynamics of a rigid body. Gos. Univ., Moscow; 1980. 241 pp.
30. Robert G. Melton, Hybrid methods for determining time-optimal, constrained spacecraft reorientation maneuves, Acta Astronautica, Volume 94, Issue 1, 2014, Pages 294-301.
31. Ilya Ioslovich, Arbitrary fuel-optimal attitude maneuvering of a non-symmetric space vehicle in a vehicle-fixed coordinate frame, Automatica, Volume 39, Issue 3, 2003, Pages 557-562

32. Jaime Rubio Hervas, Mahmut Reyhanoglu, Thrust-vector control of a three-axis stabilized upper-stage rocket with fuel slosh dynamics, Acta Astronautica, Volume 98, 2014, Pages 120-127
33. Suman Chakravorty and Jaime Ramirez, Fuel Optimal Maneuvers for Multispacecraft Interferometric Imaging Systems, Journal of Guidance, Control, and Dynamics, Vol. 30, No. 1 (2007), pp. 227-236.
34. W. E. Vander Velde and J. He, Design of space structure control systems using on-off thrusters, Journal of Guidance, Control, and Dynamics, Vol. 6, No. 1 (1983), pp. 53-60.
35. A. D. Challoner, Determination of spacecraft liquid fill fraction, AIAA Guidance, Navigation and Control Conference, Monterey, CA, Aug. 9-11, 1993, Technical Papers. Pt. 1 (A93-51301 22-63), p. 254-264.
36. V. Coverstone-Carroll, J. E. Prussing, Optimal cooperative power-limited rendezvous with propellant constraints, 1992 AIAA/AAS Astrodynamics Conference, Hilton Head Island, SC, Aug. 10-12, 1992, Technical Papers (A92-52051 22-13). Washington, American Institute of Aeronautics and Astronautics, 1992, p. 246-255.
37. Mauro Massari and Franco Bernelli-Zazzera, Optimization of Low-Thrust Reconfiguration Maneuvers for Spacecraft Flying in Formation, Journal of Guidance, Control, and Dynamics, Vol. 32, No. 5 (2009), pp. 1629-1638.
38. B. Wie and P. M. Barba, Quaternion feedback for spacecraft large angle maneuvers, Journal of Guidance, Control, and Dynamics, Vol. 8, No. 3 (1985), pp. 360-365.
39. John I. Hochstein, Alfredo E. Patag, T. P. Korakianitis, and David J. Chato, Pulsed thrust propellant reorientation - Concept and modeling, Journal of Propulsion and Power, Vol. 8, No. 4 (1992), pp. 770-777.
40. Karl D. Bilimoria and Bong Wie, Time-optimal three-axis reorientation of a rigid spacecraft, Journal of Guidance, Control, and Dynamics, Vol. 16, No. 3 (1993), pp. 446-452.
41. Wenchuan Cai, Xiaohong Liao, and David Y. Song, Indirect Robust Adaptive Fault - Tolerant Control for Attitude Tracking of Spacecraft, Journal of Guidance, Control, and Dynamics, Vol. 31, No. 5 (2008), pp. 1456-1463.
42. B. Wie and C. T. Plescia, Attitude stabilization of flexible spacecraft during stationkeeping maneuvers, Journal of Guidance, Control, and Dynamics, Vol. 7, No. 4 (1984), pp. 430-436.
43. Edward Wong, William Breckenridge, An attitude control design for the Cassini spacecraft, American Institute of Aeronautics and Astronautics, AIAA-95-3274-CP
44. Advances in Spacecraft Technologies (Collection of articles), Edited by Jason Hall, InTech (2011), 596 p.